



WONOE appraisals: Imaging biomarkers in epilepsy

*Erwin A. van Vliet, †Stefanie Dedeurwaerdere, ‡Andrew J. Cole, §¶Alon Friedman, #Matthias J. Koepp, **Heidrun Potschka, ††Riikka Immonen, ††Asla Pitkänen, and ‡‡Paolo Federico

Epilepsia, 58(3):315–330, 2017

doi: 10.1111/epi.13621



Dr. Erwin A. van Vliet is a postdoctoral researcher at the Academic Medical Center, Amsterdam.

SUMMARY

Neuroimaging offers a wide range of opportunities to obtain information about neuronal activity, brain inflammation, blood–brain barrier alterations, and various molecular alterations during epileptogenesis or for the prediction of pharmacoresponsiveness as well as postoperative outcome. Imaging biomarkers were examined during the XIII Workshop on Neurobiology of Epilepsy (XIII WONOE) organized in 2015 by the Neurobiology Commission of the International League Against Epilepsy (ILAE). Here we present an extended summary of the discussed issues and provide an overview of the current state of knowledge regarding the biomarker potential of different neuroimaging approaches for epilepsy.

KEY WORDS: Biomarker, Epileptogenesis, Traumatic brain injury, Imaging, Inflammation, Blood–brain barrier.

Neuroimaging has accelerated our knowledge of the brain and plays an important role in the diagnosis and treatment of patients with epilepsy. Using techniques such as positron

emission topography (PET) and magnetic resonance imaging (MRI), one can noninvasively study molecular, structural, and functional changes within the brain. During the Workshop on Neurobiology of Epilepsy (XIII WONOE), organized in 2015 by the Neurobiology Commission of the International League Against Epilepsy (ILAE), the focus was on neuroimaging biomarkers. Identification and proper validation of biomarkers of epileptogenesis (the development of epilepsy) and ictogenesis (the propensity to generate spontaneous seizures) might predict the development of an epilepsy condition. These biomarkers might also identify the presence and ability of tissue capable of generating spontaneous seizures, measure progression after the condition is established, and determine pharmacoresistance.¹ Furthermore, biomarkers may be used to create animal models for more cost-effective screening of potential antiepileptogenic and antiictogenic drugs and devices, and reduce the cost of clinical trials of potential antiepileptogenic interventions by enriching the trial population with patients at high risk for developing epilepsy. Research over the last decade has identified potential biomarkers for epileptogenesis and/

Accepted October 31, 2016; Early View publication November 24, 2016.

*Department of (Neuro)Pathology, Academic Medical Center, University of Amsterdam, Amsterdam, The Netherlands; †Department of Translational Neurosciences, University of Antwerp, Wilrijk, Belgium; ‡Department of Neurology, Massachusetts General Hospital, Boston, Massachusetts, U.S.A.; §Department of Brain and Cognitive Sciences, Zlotowski Center for Neuroscience, Ben-Gurion University of the Negev, Beer Sheva, Israel; ¶Department of Medical Neuroscience, Dalhousie University, Halifax, Nova Scotia, Canada; #Department of Clinical and Experimental Epilepsy, UCL Institute of Neurology, London, United Kingdom; **Institute of Pharmacology, Toxicology and Pharmacy, Ludwig-Maximilian-University, Munich, Germany; ††Department of Neurobiology, A I Virtanen Institute for Molecular Sciences, University of Eastern Finland, Kuopio, Finland; and ‡‡Departments of Clinical Neurosciences and Radiology, Hotchkiss Brain Institute, University of Calgary, Calgary, Alberta, Canada

Address correspondence to Erwin A. van Vliet, Department of (Neuro) Pathology, Academic Medical Center, University of Amsterdam, Meibergdreef 9, 1105 AZ Amsterdam, The Netherlands. E-mail: e.a.vanvliet@uva.nl

Wiley Periodicals, Inc.

© 2016 International League Against Epilepsy

KEY POINTS

- Potential neuroimaging biomarkers for epileptogenesis, ictogenesis, seizure-onset zone or postsurgery outcome are discussed:
- Positron emission tomography for neuronal hyperexcitability, brain inflammation, and drug response
- Contrast-enhanced magnetic resonance imaging for blood–brain barrier dysfunction
- Magnetic resonance spectroscopy and magnetic resonance imaging for metabolic and structural abnormalities
- Functional magnetic resonance imaging for language and memory decline after surgery and epileptiform discharges

or ictogenesis, including neuroimaging markers.^{1,2} In this article, we provide an overview of the current state-of-art knowledge of neuroimaging biomarkers for epileptogenesis or ictogenesis related to brain inflammation, blood–brain barrier (BBB) dysfunction, epileptogenic lesions, as well as the irritative and seizure-onset zones (Table 1) In addition, we provide an extended summary of the issues that were discussed during the XIII WONOEP. Imaging methods to be discussed will include PET and advanced MR methods such as contrast-enhanced imaging, spectroscopy, and T2 relaxometry in animal models of epileptogenesis and in the human epileptic brain (Fig. 1). Furthermore, we discuss recent advances in identifying the irritative zone (e.g., scalp and intracranial electroencephalography–functional MRI [EEG-fMRI]) as well as the seizure-onset zone (ictal fMRI and arterial spin-labeling MRI). Finally, we review recent MRI advances in the study of the negative consequences of epilepsy on some aspects of neurocognitive function, focusing on structural and functional MRI connectivity.

POSITRON EMISSION TOMOGRAPHY

PET biomarkers of epileptogenesis, the epileptogenic zone, and status epilepticus

¹⁸F-Fluorodeoxyglucose (FDG) is a radiolabeled analogue of glucose. FDG uptake from the blood to the brain is mediated by glucose transporters. In the brain it is phosphorylated by hexokinase into FDG-6-P, which is semipermanently trapped in cells and not further metabolized (Fig. 2).

From studies in post status epilepticus (SE) models it became evident that hypometabolism is present early during epileptogenesis, from 12 to 48 h after SE.^{3,4} More severe hypometabolism during epileptogenesis was associated with a higher seizure burden in the pilocarpine-induced SE model and higher risk for epilepsy in the lateral fluid-percussion injury (LFPI) model for traumatic brain injury.^{4,5}

The utility of FDG-PET in patients with epilepsy was first described in a series of reports in the late 1970s/early 1980s^{6,7} demonstrating focal ictal hypermetabolism and interictal hypometabolism that co-localized with the epileptogenic zone. These findings have been reproduced many times thereafter.⁸ More recently, single-photon emission computed tomography (SPECT) studies using labeled lipophilic tracers such as technetium hexamethylpropyleneamine oxime (⁹⁹Tc-HMPAO) reliably demonstrate ictal hyperperfusion when injected during seizures and variable hypoperfusion when injected postictally or interictally.⁸ The strong increase in FDG uptake and perfusion during seizures, representing glucose hypermetabolism and blood flow, respectively, is most elegantly conceptualized as a biomarker of increased neuronal activity resulting, in the appropriate clinical context, from underlying neuronal hyperexcitability (Fig. 2).

A major challenge in the clinic is defining SE and differentiating it from nonepileptic causes of altered mental status. This problem is particularly acute in critically ill patients with neurologic injury who may be in nonconvulsive SE. Traditional definitions of SE have relied heavily on EEG criteria including clearly evolving events or repetitive epileptiform discharges. Repetitive epileptiform discharges may be seen in a variety of settings as a nonspecific marker of neuronal injury that is unlikely to be epileptic, such as Creutzfeldt-Jakob disease, metabolic encephalopathy, and ischemic stroke. Because there is no gold standard for establishing a diagnosis of nonconvulsive SE, EEG-based definitions have been largely adopted, but the true significance of repetitive discharges in these states has been debated briskly in the clinical literature.^{9,10} FDG-PET offers another potential biomarker of SE that relies on the presence or absence of increased metabolic activity consistent with increased neuronal activity to complement EEG-based definitions. In a series of 18 patients with possible or probable SE based solely on EEG criteria, FDG-PET hypermetabolism correctly classified those in status with 80% sensitivity and 100% specificity, supporting the use of PET as an orthogonal biomarker of SE.¹¹ Figure 3 provides examples of an equivocal EEG pattern with co-localized FDG-PET hypermetabolism that resolved with anticonvulsant treatment, and an EEG pattern suggestive of SE with occipital hypometabolism in a patient with Creutzfeldt-Jakob disease who did not respond clinically to anticonvulsant drug treatment. This indicates that FDG-PET can be a biomarker of SE. An epileptogenesis biomarker for stratifying patients at risk would be valuable for clinical trials investigating antiepileptogenesis treatment strategies. However, additional preclinical and clinical studies are required to investigate whether FDG-PET has the sensitivity and selectivity as a predictive biomarker of epileptogenesis.

Recently, several groups have started to investigate the role of brain inflammation in epileptogenesis. PET ligands targeting translocator proteins (TSPOs) have been

Table 1. Overview of neuroimaging studies and their biomarker potential

Modality	Tracer/parameter	Human/animal model	Biomarker	References
FDG-PET	¹⁸ F-FDG	Rat pilocarpine SE model Rat lateral fluid percussion injury model	Epileptogenesis	4,5
FDG-PET	¹⁸ F-FDG	Human (temporal lobe) epilepsy and SE	Ictogenesis and SE	6–8,11
SPECT	⁹⁹ Tc-HMPAO	Human temporal lobe epilepsy	Ictogenesis and seizure-onset zone	8
TSPO-PET	¹⁸ F-PBR111 or ¹¹ C-PK11195	Rat kainic-acid SE model	Ictogenesis	14–16
TSPO-PET	¹¹ C-PK11195	Rat amygdala electrical stimulation SE model	Response to phenobarbital	23
TSPO-PET	¹¹ C-PBR28 or ¹¹ C-DPA-713	Human temporal lobe epilepsy	Seizure-onset zone	20,21
Pgp-PET	¹⁸ F-MPPF + tariquidar or ¹¹ C-quinidine + tariquidar	Rat amygdala electrical stimulation SE model	Response to phenobarbital	26,27
Pgp-PET	(R)-[¹¹ C]verapamil with and without tariquidar	Human temporal lobe epilepsy	Response to AEDs	30,31
Pgp-PET	(R)-[¹¹ C]verapamil with cyclosporine A	Human frontal lobe and temporal lobe epilepsy	Response to AEDs	32
CE-MRI	Gadolinium-DTPA	Rat kainic-acid SE model	Ictogenesis	43,44
CE-MRI	Gadolinium-DTPA	Human traumatic brain injury	Ictogenesis	47
¹ H-MRS	Glutathione and myo-inositol	Rat kainic-acid SE model	Epileptogenesis (glutathione), neuronal damage (glutathione and myo-inositol)	51
¹ H-MRS	NAA/Cr ratio	Human temporal lobe epilepsy	Postsurgery outcome	55,56
¹ H-MRS	NAA/tCr	Human epilepsy	Seizure onset zone and AED response	49,50
¹ H-MRS	Myo-inositol	Human temporal lobe epilepsy	Seizure onset zone	57
MRI	T2	Rat febrile seizure model	Epileptogenesis	64
MRI	T2, Dav, T1 rho	Rat lateral fluid percussion model for TBI	Seizure susceptibility	63,65
EEG-fMRI	Interictal epileptiform discharges and BOLD response	Rat focal cortical dysplasia model	Topological properties of resting state network	68
EEG-fMRI	Interictal epileptiform discharges and BOLD response	Human focal epilepsy	Irritative or seizure onset zone	69–74,78
EEG-fMRI	Interictal epileptiform discharges and BOLD response	Human focal epilepsy	Postsurgery outcome	75,76
ASL-MRI	Cerebral blood flow	Rat pilocarpine SE model	Seizure onset zone	80
ASL-MRI	Cerebral blood flow	Human focal epilepsy	Seizure onset zone	81,82
fMRI	Verbal, auditory or visual memory paradigms	Human temporal lobe epilepsy	Verbal, auditory, or visual memory after resection	88,89,91,93
fMRI	Working memory paradigm	Human temporal lobe epilepsy	Working memory after resection	95

AEDs, antiepileptic drugs; ASL, arterial spin labeling; BOLD, blood oxygen level dependent; CE-MRI, contrast-enhanced magnetic resonance imaging; Cr, creatine; Dav, mean diffusivity; EEG, electroencephalography; FDG, fluorodeoxyglucose; fMRI, functional magnetic resonance imaging; HMPAO, hexamethylpropyleneamine oxime; NAA, N-acetylaspartate; MRS, magnetic resonance spectroscopy; PET, positron emission tomography; SPECT, single-photon emission computed tomography; SE, status epilepticus; tCr, total creatine; TSPO, translocator protein; Pgp, P-glycoprotein.

developed to investigate neuroinflammation in vivo (Fig. 2) and provide a tool to perform longitudinal follow-up studies.¹² Under inflammatory conditions, TSPO, a mitochondrial protein, is up-regulated, whereas under normal conditions its expression is low. It has been shown that TSPO expression in epilepsy models is related predominantly to the activated status of microglia.^{13–15} Studies investigating the expression of TSPOs in vivo during epileptogenesis revealed that TSPO expression and microglia activation is particularly high during the latent phase in the kainic acid-induced post-SE model,^{14–16} suggesting that TSPO can be a biomarker of brain inflammation and epileptogenesis. Brain inflammation has been proposed to have perpetuating effects on brain excitability and seizure generation.¹⁷ Markers of microglia and astrocyte activation are increased in experimental models and brain tissue of patients with epilepsy, which is paralleled by TSPO overexpression. More interesting, a positive correlation between

TSPO expression and the number of seizures has been found in the kainic-acid post-SE model.¹⁵ These results suggest that TSPO is a noninvasive biomarker of brain inflammation, epileptogenesis, and/or ictogenesis; however, this needs to be investigated in further detail.

TSPO may also be a biomarker for drug response. In a rat stroke model, it has been shown that TSPO-PET can detect the antiinflammatory effect of minocycline when administered shortly after stroke.¹⁸ In this study, minocycline was preventing the strong inflammatory response following stroke. In the experimental autoimmune encephalitis model, fingolimod treatment reduced TSPO-PET binding and microglia activation.¹⁹ An important step will be to investigate whether successful antiinflammatory treatment of chronic neuroinflammation in epilepsy models is reflected by a reversal of TSPO expression.

PET studies using ¹¹C-PK11195 showed increased in vivo TSPO binding in patients with epilepsy (for review

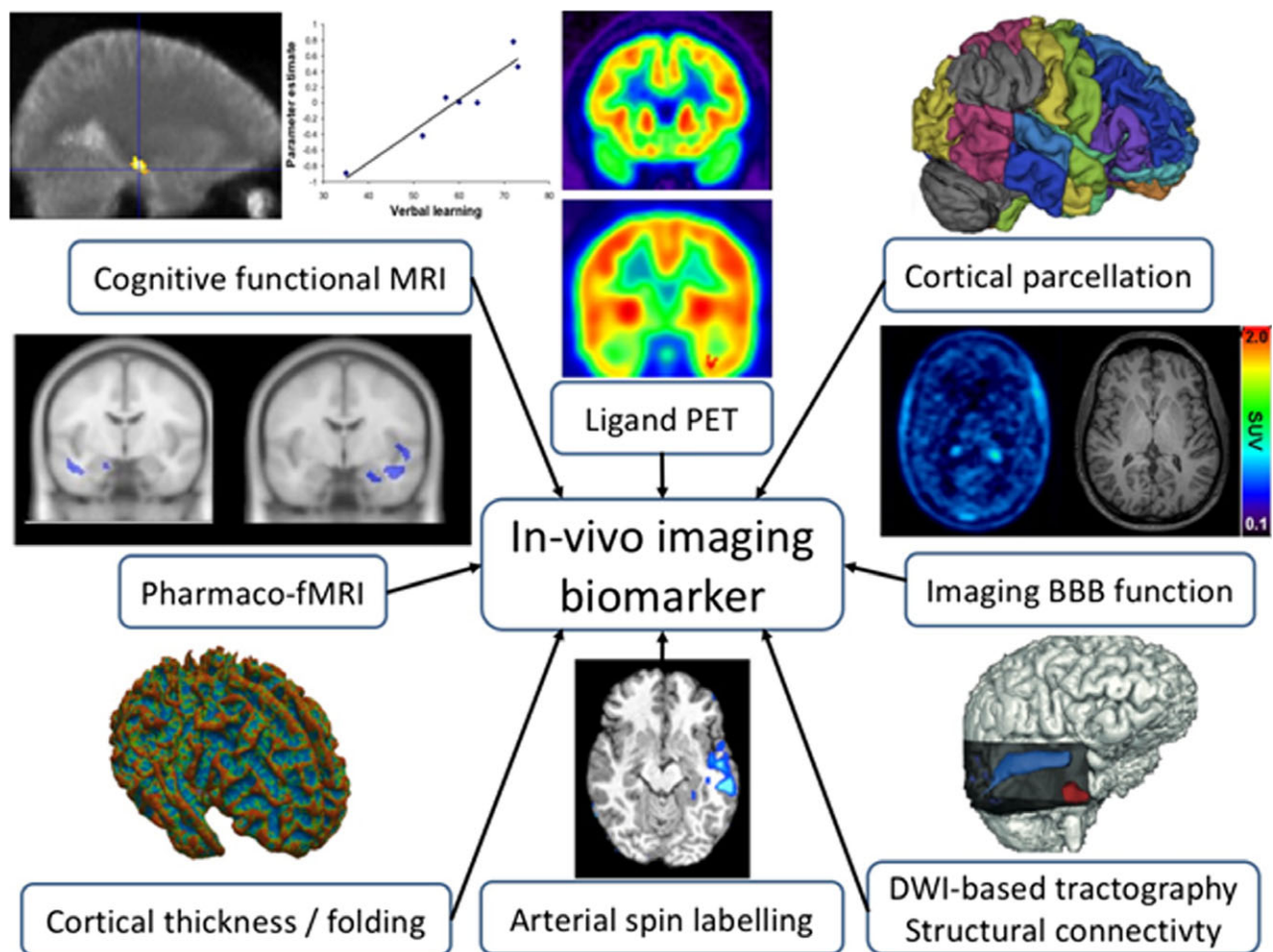


Figure 1.

Summary of advanced MRI methods used in the study of epilepsy. Clockwise from top left: correlation of fMRI memory activations in the anterior hippocampus with performance in verbal learning; increased mesiotemporal uptake of 18F-GE179 showing increased N-methyl-D-aspartate (NMDA) activation; atlas used for cortical parcellation and volume-of-interest analysis; ^{11}C -verapamil PET reflecting P-glycoprotein activity/BBB function; tractography of optic radiation; ASL in temporal lobe epilepsy; three-dimensional (3D) presentation of cortical thickness and folding pattern; effect of levetiracetam on working memory fMRI-activation patterns.

Epilepsia © ILAE

see Amhaoul et al.¹²). More recently, second generation TSPO ligands with higher signal-to-noise ratio were used in patients with TLE.^{20,21} These studies found increased TSPO binding, particularly ipsilateral to the seizure-onset zone (SOZ). On the other hand, a relationship between TSPO increase and seizure frequency was not demonstrated in patients, whereas this has been observed previously with TSPO autoradiography in a preclinical study.¹⁵ Furthermore, some TSPO ligands have binding sensitivity to a human single nucleotide polymorphism rs6971, which imposes limitations on their utility for comparative quantitative PET studies of normal and diseased subjects.²² Nevertheless, these findings provide opportunities to use TSPO-PET as a biomarker to evaluate the effect of anti-inflammatory treatments.

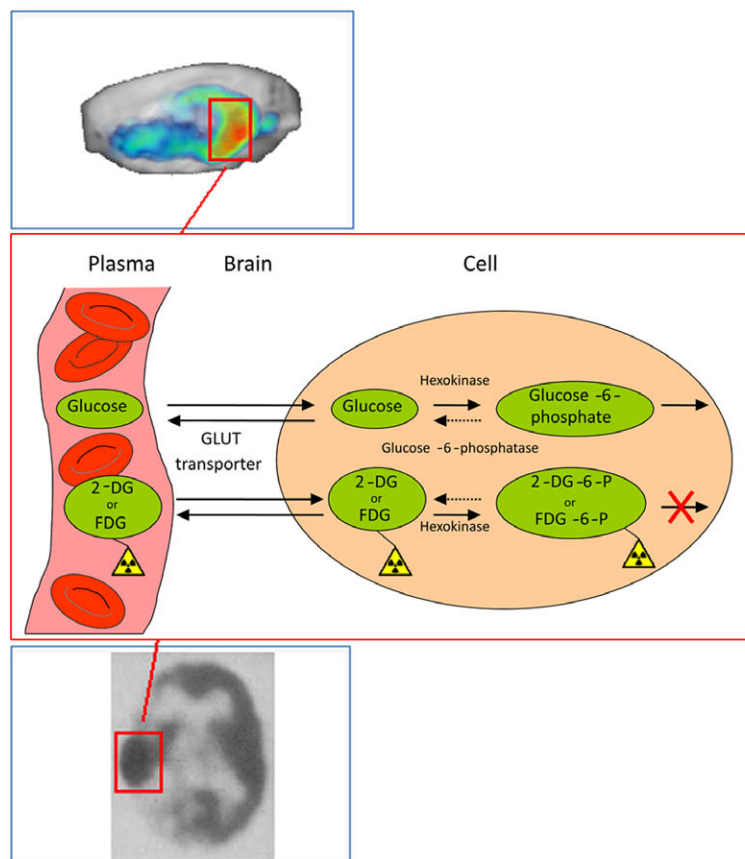
PET imaging biomarkers of drug resistance

Prediction of drug resistance is a desirable objective as it would render a basis for individualized therapeutic decisions. On one hand it might guide the straightforward selection of therapeutic management approaches and avoid therapeutic trials that are deemed to fail. On the other hand, respective biomarkers might also help to diagnose multidrug resistance early on, thereby promoting early decisions for nonpharmacologic approaches. In this context it is of utmost importance to assess whether a biomarker renders information about drug resistance and does not merely reflect intrinsic severity and seizure frequency.

An experimental study selected rats with spontaneous recurrent seizures based on their response to phenobarbital

Neuronal activity

status epilepticus visualized with FDG PET

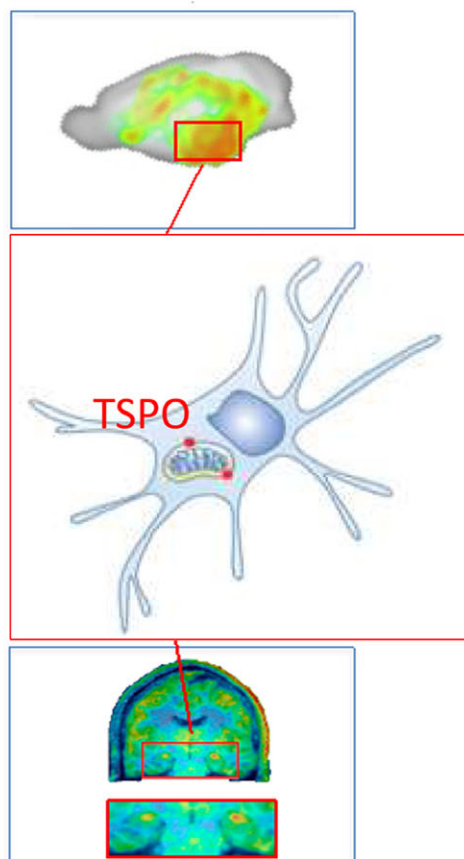


Biomarker

- of status epilepticus
- for resection of the epileptogenic zone
- of epileptogenesis (needs clinical confirmation)

Brain inflammation

microglia activation visualized with Translocator protein PET radioligand



Biomarker

- of seizure burden (needs clinical confirmation)
- for anti-inflammatory treatment (needs preclinical and clinical evidence)
- of epileptogenesis (needs preclinical and clinical evidence)

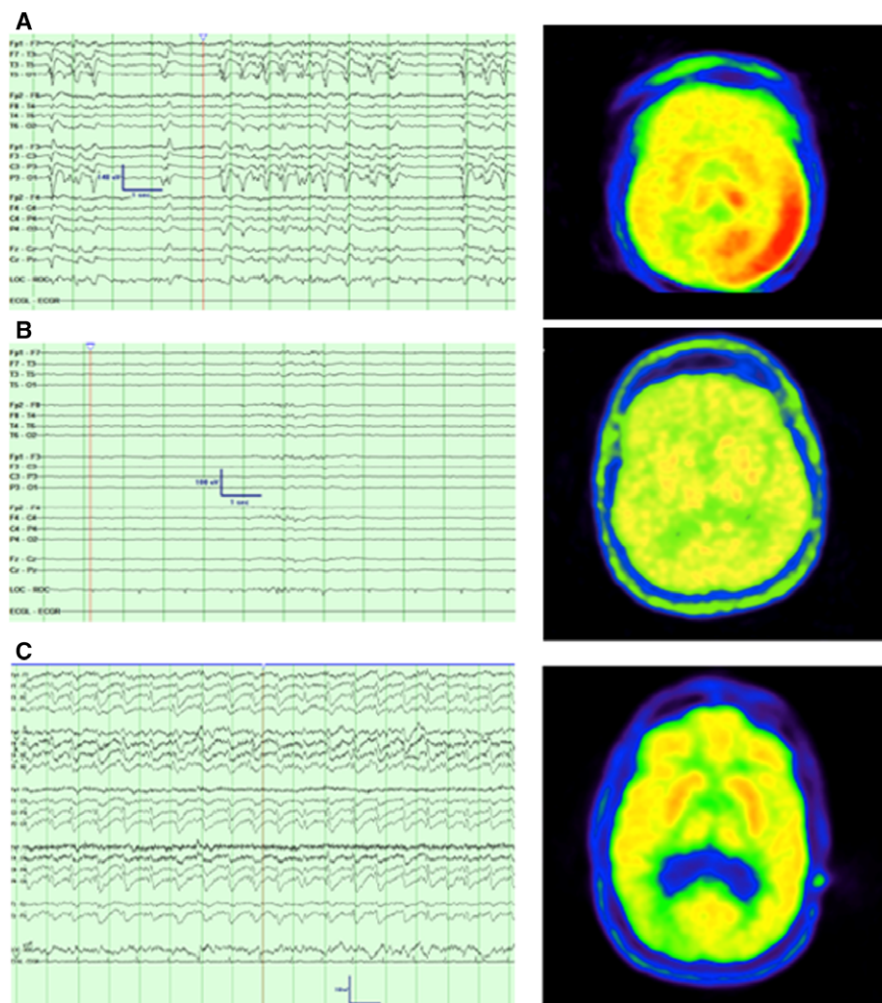
Figure 2.

PET imaging biomarkers of epilepsy. Imaging of FDG-PET (left panels) and TSPO (right panels) in the rat kainic acid-induced SE model (top panels, 3D-rendered images, sagittal view) and in patients with TLE (bottom panel). ^{18}F -FDG, an analogue of glucose, is injected intravenously or intraperitoneally and will enter the brain through GLUT-mediated transport. Next, it will be phosphorylated and trapped intracellularly representing cerebral glucose utilization. FDG scans in rat and human are taken during SE demonstrating a strong FDG increase particularly in the limbic regions and ventral striatum in rat (upper left) and perisylvian area of a TLE patient (bottom left, Engel et al.,⁷ reprinted with permission from AAAS). TSPO PET ligands bind to TSPO which is overexpressed under inflammatory conditions, particularly on mitochondria of activated microglia but to a lesser extent also astrocytes. ^{18}F -PBR111 uptake is strongly increased in limbic brain regions in the rat 2 weeks post-SE (upper right). In a TLE patient, ^{11}C -PBR28 was increased in the ipsilateral hippocampus (fused PET/MRI image) (Hirvonen et al.,²⁰ ©by the Society of Nuclear Medicine and Molecular Imaging, Inc.).

Epilepsia © ILAE

administration.²³ The analysis assessed the difference between phenobarbital responders and nonresponders in the uptake of the TSPO tracer (R)- ^{11}C PK11195. In nonresponders, increased brain uptake of the tracer was evident in

different brain regions, which are involved in generation and spread of seizure activity in the rat model of temporal lobe epilepsy (TLE).²³ Of interest, comparison of rats with drug-sensitive epilepsy with electrode-implanted control

**Figure 3.**

FDG-PET studies in patients with possible SE. (A) EEG shows irregular left posterior quadrant epileptiform spikes in a patient with focal hypermetabolism suggesting focal SE. (B) After treatment with anticonvulsant medications EEG pattern resolves and PET normalizes. (C) EEG shows regular continuous repetitive epileptiform discharges at approximately 1.25 Hz maximal in the right posterior quadrant in a patient with focal hypometabolism in the same region. These findings and the patient's evolution led to a diagnosis of Heidenhain variant of Creutzfeldt-Jakob disease. This indicates that FDG-PET can be a biomarker of SE.

Epilepsia © ILAE

rats did not reveal relevant differences. This fact might be related to the restricted affinity and sensitivity of the TSPO tracer [^{11}C]PK11195. A correlation with baseline seizure frequency was observed only in the hippocampus, when data from the complete scanning phase including the early influx phase were considered, but not when a time frame of 20–60 min of the scan was assessed.²³ Thus, the data support the hypothesis that TSPO imaging might be suitable for prediction of drug responses. However, future experimental and clinical studies are required to further investigate the biomarker potential of TSPO in the context of drug-resistant epilepsy. In particular, one needs to determine the correlation between TSPO expression and response to different antiepileptic drugs.

Alterations at the BBB might affect antiepileptic drug brain penetration and efficacy. Research has focused on the impact of multidrug transporters on brain access of antiepileptic drugs. The current state of knowledge indicates that the seizure-associated up-regulation of P-glycoprotein might influence different antiepileptic drugs or their metabolites. Strong efforts have been made to

develop PET-imaging approaches to determining the expression and/or function of P-glycoprotein.^{24,25} The general concept of these approaches developed during an EU-funded project coordinated by Matthias Koepp was based on the combination of radiotracers that serve as substrates of P-glycoprotein with modulators of transporter function. Investigations in the rat model of drug-resistant TLE suggested that the concept might be generally suited for prediction of drug responses.²⁶ Pretreatment of rats with a relatively high dose of the P-glycoprotein modulator tariquidar increased the tracer influx and efflux rates in a more pronounced manner in nonresponder rats.

Alternate tracers for imaging of P-glycoprotein function have been assessed experimentally. Analysis in a rat model of drug-resistant epilepsy confirmed that [^{11}C]quinidine and [^{11}C]laniquidar are substrates of P-glycoprotein.²⁷ However, only slight differences were determined for [^{11}C]quinidine, when comparing data from animals with drug-resistant and drug-sensitive epilepsy.

As a matter of course, experimental proof-of-concept studies do not always allow direct translation to patients. As an example, 2'-methoxyphenyl-(*N*-2'-pyridinyl)-p-18F-fluoro-benzamidoethylpiperazine ($[^{18}\text{F}]\text{MPPF}$) is a substrate of rodent P-glycoprotein, but it does not seem to be transported by the human P-glycoprotein isoform.²⁸ Thus, clinical studies have focused on the use of alternate P-glycoprotein substrate radiotracers.

In vitro transport experiments confirmed that (R)- $[^{11}\text{C}]$ verapamil is selectively transported by human P-glycoprotein, but not by multidrug-resistance protein 1 and breast cancer resistance protein.²⁹ Feldmann et al.³⁰ have completed a case-control study in patients with TLE. Brain uptake of (R)- $[^{11}\text{C}]$ verapamil was higher in patients with drug-sensitive epilepsy than in patients with drug-resistant epilepsy. The difference in the uptake was evident in the temporal lobe of the ipsilateral and contralateral sides.³⁰ These findings are consistent with an overexpression of P-glycoprotein and enhanced transport function in drug-resistant epilepsy. Partial inhibition was achieved by pretreatment with a low dose of tariquidar in a separate set of scans in patients with drug-resistant epilepsy and healthy controls. The effect of tariquidar proved to be attenuated in patients with poor drug responses, with the ipsilateral hippocampus most significantly affected.³¹ It was concluded that the findings are in line with enhanced P-glycoprotein function in drug-resistant epilepsy with partial inhibition of P-glycoprotein resulting in less-pronounced relative effects.³⁰

A follow-up study assessed a combination of (R)- $[^{11}\text{C}]$ verapamil with the P-glycoprotein modulator cyclosporin A in a simultaneous PET/MRI approach.³² The authors reported that the asymmetry indices of the tracer uptake values proved to be comparable between healthy controls and patients with drug-sensitive epilepsy, whereas data from patients with drug-resistant epilepsy obviously differed from those of the other groups.

Alternate tracers for imaging of P-glycoprotein function have been assessed clinically. $[^{11}\text{C}]\text{-}N\text{-Desmethyl-loperamide}$ proved to be significantly affected by P-glycoprotein function at the human BBB.^{33,34} However, recent data demonstrated that $[^{11}\text{C}]\text{-}N\text{-desmethyl-loperamide}$ metabolism is altered by isoflurane anesthesia and that its brain distribution is affected by cerebral blood flow, whereas no such influence was observed for (R)- $[^{11}\text{C}]$ verapamil.³⁵ Thus, from the current state of knowledge, (R)- $[^{11}\text{C}]$ verapamil and tariquidar might serve as the best available option for imaging of P-glycoprotein.

Whereas experimental and clinical data suggest that imaging of P-glycoprotein might help to predict drug responsiveness in TLE, further studies are necessary to confirm the validity as a reliable biomarker that renders valuable supplementary information. Challenges are related to the fact that drug resistance is considered a multifactorial problem.

CONTRAST-ENHANCED MAGNETIC RESONANCE IMAGING FOR THE DETECTION OF BBB DYSFUNCTION

The BBB plays an important role in the homeostasis of the brain. Specialized endothelial cells that are connected via tight junctions and specific transport systems control brain extracellular environment and protect the brain from potentially harmful substances in the bloodstream. BBB dysfunction that results in the entry of blood components to the brain extracellular space is observed in several disorders of the central nervous system, including epilepsy.³⁶ BBB dysfunction can have important consequences for neuronal excitability and can therefore be involved in the generation of seizures and epilepsy. There is ample evidence from experimental animal studies that BBB dysfunction can be caused by seizure activity.³⁷⁻³⁹ However, research in the last decade shows that BBB dysfunction can also lead to epilepsy or aggravate the epileptic condition.

Longitudinal in vivo imaging studies,⁴⁰ including contrast-enhanced MRI (CE-MRI), can be used to study BBB dynamics during epileptogenesis and may be of importance for the assessment of future therapies, including those targeting the BBB. Gadolinium (Gd)-based MR contrast agents such as Gd-diethylenetriaminepentaacetate (Gd-DTPA) can be used to detect BBB dysfunction. When the BBB is disrupted, the intravenously administered MR contrast agent leaks out of the blood vessels and accumulates in brain parenchyma. This results in local shortening of the longitudinal MR relaxation time, T₁. The changes in MR signal can be used to localize BBB disruption and to quantify the relative degree of BBB permeability. A recent study in the kainic acid-induced post-SE rat model showed that with longitudinal CE-MRI in combination with a steady-state infusion of gadobutrol it is possible to detect and quantify BBB leakage using T₁-weighted MRI (*post-pre approach*) and T₁ mapping (*dynamic approach*).⁴¹ In the *post-pre approach* the differences between T₁-weighted MRI scans before and after tracer infusion are calculated, whereas the *dynamic approach* with fast T₁ mapping detects dynamic changes during tracer infusion. Previous CE-MRI studies failed to detect BBB leakage during epileptogenesis in similar rat models,^{3,42} which may be explained by the fact that MR contrast agents were given as bolus injections in these studies, which do not provide sufficient and steady-state blood levels.

In a recent study, the effects of the immunosuppressant rapamycin were investigated on BBB permeability using CE-MRI in combination with a steady-state infusion of gadobutrol and on epileptogenesis in the kainic-acid post-SE rat model.⁴³ Widespread and extensive leakage of the BBB tracer gadobutrol was observed in both rapamycin and vehicle-treated epileptic rats during the acute and latent phase with the piriform cortex and amygdala as the most

affected regions (Fig. 4A). Higher gadobutrol leakage is evident in rapamycin-treated rats 4 and 8 days after SE compared to vehicle-treated rats (Fig. 4A,B), indicating a slower recovery of the SE-induced BBB disruption by rapamycin treatment. However, less gadobutrol leakage is observed during the chronic epileptic phase (3 and 6 weeks after SE) in rapamycin-treated epileptic rats (Fig. 4A,B) along with a decreased seizure frequency. This is paralleled by reduced local blood vessel density, activated microglia, and astrogliosis in rapamycin-treated rats compared to vehicle-treated rats,⁴⁴ suggesting that rapamycin more quickly resolves inflammation and improves BBB function after wound healing. The extent of gadobutrol leakage at early time points did not correlate with seizure activity in the chronic phase (Fig. 4C), which indicates that BBB leakage measured with CE-MRI in the kainic-acid post-SE model cannot be used as biomarker that will predict severity of future seizures. In contrast, at 6–7 weeks after SE, gadobutrol leakage is correlated positively with the number of seizures at the chronic stage (Fig. 4D), suggesting that BBB leakage measured with CE-MRI during the chronic phase could be used as a diagnostic biomarker for disease activity and as a potential pharmacodynamics biomarker to monitor therapeutic efficacy. This is also supported by previous studies in rats with recurrent seizures.^{37,41}

Although CE-MRI is used routinely in humans, quantitative imaging of BBB permeability in humans has not been implemented in routine clinical settings due to complicated and demanding dynamic scanning protocols, including tracer injection during scanning and long scanning sessions.⁴⁵ As the understanding of the critical role of the BBB in brain pathologies continues to advance, the need for the establishment of practical BBB imaging methods in clinical settings is becoming urgent. Chassidim et al.⁴⁶ showed that BBB leakage can be quantified using the *post-pre approach*, as well as with the *dynamic approach* in humans (Fig. 5). Tomkins et al.⁴⁷ investigated 37 patients with mild to moderate traumatic brain injury and showed using CE-MRI and quantitative EEG analysis that patients with posttraumatic epilepsy are more likely than posttraumatic patients without epilepsy to show abnormal BBB permeability. These results further support a role for microvascular pathology, specifically BBB dysfunction, in the pathogenesis of posttraumatic epilepsy.

Because BBB opening per se may lead to the induction of epileptogenesis and promote the generation of seizures, BBB permeability may serve as a candidate biomarker for epileptogenesis.⁴⁸ Furthermore, modulation of BBB permeability could have a therapeutic value. Therefore, future studies are required to further confirm the potential of BBB functional status as a diagnostic, predicting, and pharmacodynamics biomarker for epileptogenesis and seizures. Thus, testing of BBB imaging during epileptogenesis and its potential to predict antiepileptogenic effects of new BBB or antiepileptogenic drugs requires further studies.

STRUCTURAL AND FUNCTIONAL IMAGING

MRI and magnetic resonance spectroscopy (MRS) provide tools to noninvasively probe the abnormalities in neuronal networks and their chemical composition at a given time point during epileptogenic process both in humans and in experimental models. Because the signals given by abnormal tissue are in general translatable from one species to another, MRI and MRS provide methodologies that can be translated from the laboratory to the clinic.

Magnetic resonance spectroscopy (MRS) as a tool to identify metabolic biomarkers for epileptogenesis

MR spectroscopy (only ¹H-MRS is discussed here) can be used to measure the levels of a set of metabolites in vivo at a given time point. One can choose to use a localized MRS in a preselected voxel of interest (VOI) and generate a quantitative tissue neurochemical profile with a single measurement of up to 21 neurochemicals. Another possibility is to map a larger portion of the brain with a grid of spectroscopy voxels by using MR spectroscopic imaging (MRSI), which, however, reduces the number of measurable neurochemicals as usually only the largest peaks such as *N*-acetylaspartate (NAA), total choline (tCho), total creatine (tCr), or lipids and lactate (Lac) are measurable even in the case of robust pathologies such as in tumor or hypoxic conditions.

The strength of MRS is that it can reveal metabolic abnormalities in brain tissue that appears normal in MRI. However, given that epileptogenesis-related metabolic abnormalities can be focal and mild, the voxel placement becomes critical to avoid false-negative findings. A recent consensus paper on the role of proton-MRS in clinical management emphasized combined use of single-voxel spectroscopy and MR spectroscopic imaging.⁴⁹ It was recommended that the localization of pathology should be done by using MRSI and the quantification of the focal neurochemical profile by short echo-time MRS. Identifiable molecules by using short echo-time MRS can be categorized into those involved in energy metabolism (e.g., lactate [Lac], creatine [Cr]), neurotransmission (e.g., glutamate [Glu], glutamine [Gln], γ -aminobutyrate [GABA]), antioxidant, and osmolysis (e.g., glutathione [GSH], taurine [Tau], myo-inositol [mIns]), as well as myelination and membrane metabolism (e.g., NAA).⁵⁰ Of interest, many of the listed molecules provide information about pathology related to epileptogenic injuries (e.g., stroke, traumatic brain injury), and presumably, contribute to epileptogenesis. Yet, MRS data monitored in experimental and clinical studies to date are often limited to NAA, Gln + Glu, mIns, GABA, PCho + GPC, and, more recently, to GSH.

Studies applying MRS to investigate epileptogenesis and epilepsy in animal models are scarce. Filibian et al.⁵¹

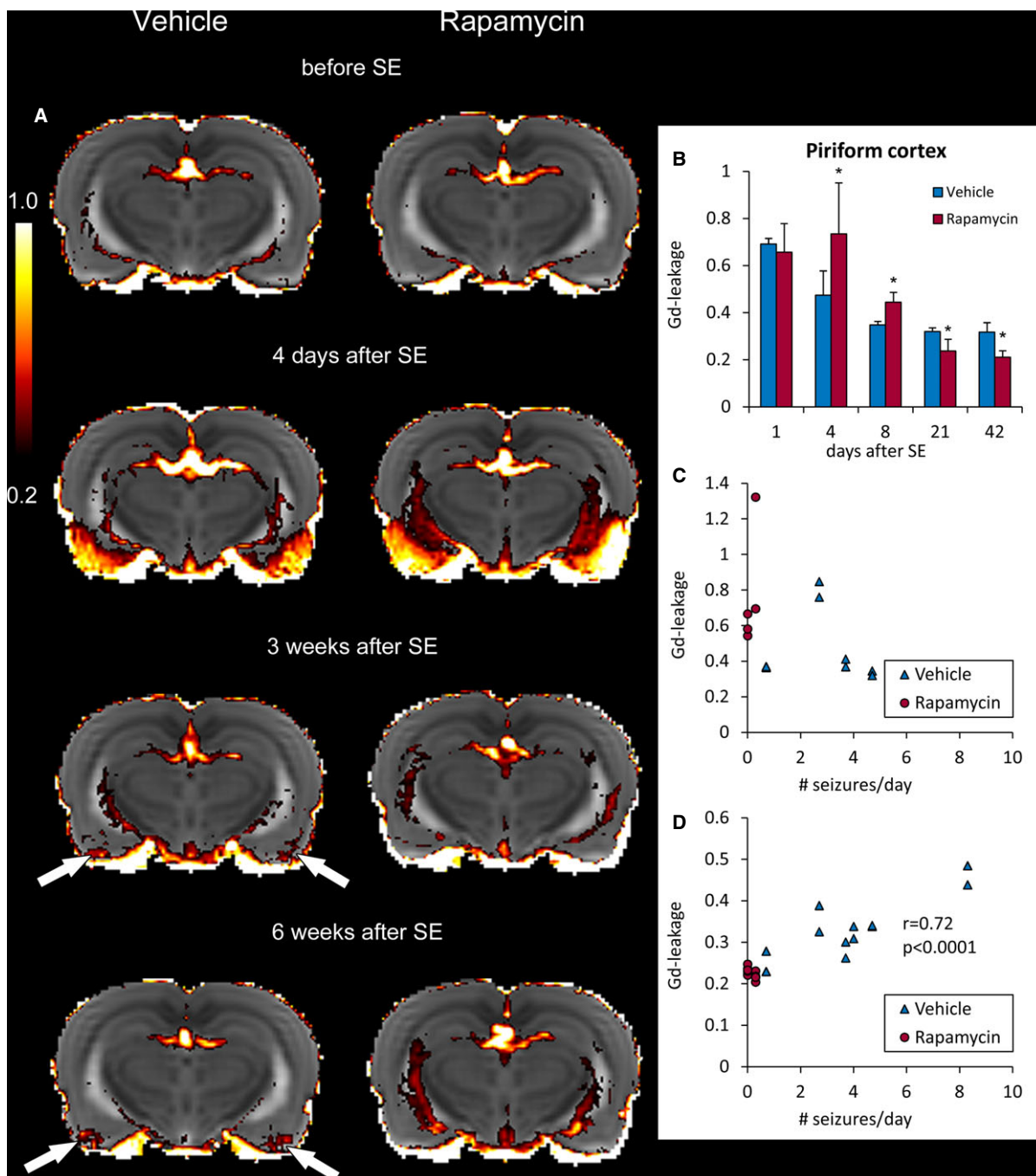


Figure 4.

BBB assessment using CE-MRI during epileptogenesis in vehicle-treated and rapamycin-treated rats. To identify brain regions with gadobutrol leakage, precontrast T_1 -weighted images were subtracted from postcontrast images and divided by precontrast images (**A**; Gd-leakage maps). No significant gadobutrol enhancement was detected in the brain before SE, except for the ventricles/circumventricular organs, which have an incomplete BBB. Gd-leakage increased bilaterally at 4 days after kainic acid-induced SE (**A** and **B**), mainly in ventral brain regions (hippocampus, entorhinal cortex, amygdala, piriform cortex, and thalamus). Partial recovery of BBB function was observed during the chronic epileptic phase, 3 and 6 weeks after SE, but Gd-leakage remained higher bilaterally (white arrows) as compared with before SE (**A** and **B**). The color bar in **A** indicates the relative Gd-leakage value. Gd-leakage that was quantified 4 days weeks after SE in the piriform cortex of vehicle-treated rats (**C**) was not correlated with the number of seizures that occurred at the seventh week after SE in those rats, indicating that Gd-leakage at this time points after SE does not predict later epilepsy. In contrast, Gd-leakage that was quantified 6 weeks after SE in the piriform cortex of the same rats (**D**) was positively correlated with the number of seizures that occurred at the seventh week after SE in those rats ($r = 0.72$, $p < 0.0001$, Pearson correlation).

Epilepsia © ILAE

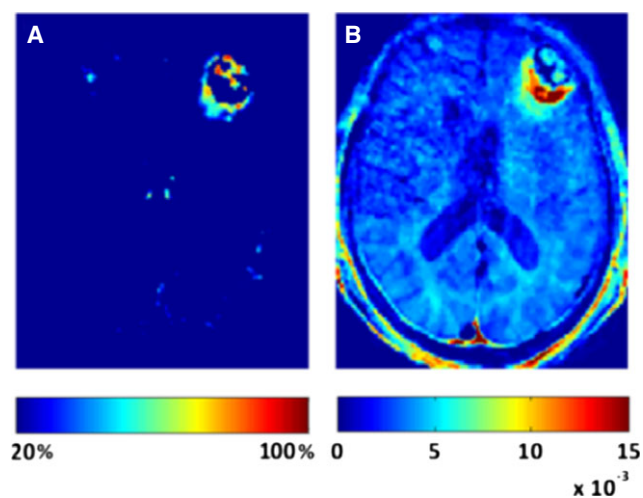


Figure 5.

BBB assessment using CE-MRI in a patient with a lesion in the left hemisphere. (A) Post-pre approach, in which a statistical comparison is performed between pre- and postcontrast agent injections (color bar = difference percentage). (B) Dynamic approach, where the dynamics of the signal change in repeated scans acquired before and after contrast agent injection are calculated, assuming a linear model (color bar = normalized slope, per second). Both methods show enhanced permeability at the margins and in the core of the lesion. Figure adapted from Chassidim et al.⁴⁶

Epilepsia © ILAE

induced epileptogenesis with kainic acid, and reported a progressive increase in astrocyte markers mIns and GSH along with NAA reduction in the hippocampus, suggesting that those markers are biomarkers for epileptogenesis. These observations had a temporal connection to tissue pathology, presenting reactive astrogliosis, microgliosis, and neurodegeneration. Of interest, the higher the GSH during epileptogenesis, the lower the seizure frequency. Moreover, the higher the S100 β level (astrocyte marker) in chronic epileptic tissue, the higher the seizure frequency, indicating that this is a biomarker for ictogenesis. Recent data using the lateral fluid-percussion injury model of TBI revealed that increased mIns in the ipsilateral hippocampus associated with the severity of memory impairment in Morris water maze (Fig. 6H) but failed to link this glia marker with electrographic epileptiform activity. It is interesting that lactate levels did not show any long-lasting increases during epileptogenesis, suggesting that reported elevations in lactate at acute postinjury stage after SE and traumatic brain injury (TBI) are apparently related to the insult itself.

MRS can also identify focal abnormalities in patients with focal epilepsy. Ipsilaterally, hippocampal NAA was reduced and Cho and Cr (lower NAA/Cho + Cr ratio) elevated in patients with hippocampal sclerosis.^{52–54} However, a correlation with postsurgical seizure freedom was less clear. One study showed that the severity of contralateral NAA/Cr ratio abnormality predicted postoperative seizure freedom. Another study, which included patients with normal MR

scans, showed that a poor surgical outcome was associated with a mildly reduced NAA/(Cho + Cr) ratio in the epileptic hippocampus.^{55,56} Although NAA/tCr levels are decreased in the focal SOZ area, the recovery of NAA (neuronal functionality marker) levels has been used as an indicator of a treatment response in clinical epilepsy management.^{49,50} Increased mIns/tCr is an indicator of gliosis. Wellard et al.⁵⁷ described mIns abnormalities in TLE patients using single-voxel MRS of the temporal and frontal lobes, and found an increase in hippocampal mIns but a reduction in frontal mIns ipsilaterally. According to Wellard's interpretation, increased mIns (together with decreased NAA) could be attributed to a SOZ, whereas reduced mIns could signal about the networks involved in seizure spread. A limited number of studies have shown that MRS may also help to identify and differentiate between various types of cortical malformations and hypothalamic hamartomas.^{58,59}

Structural MRI as a tool to identify biomarkers for epileptogenesis

High-resolution structural MRI (or μ MRI) is the only in vivo technique capable of identifying a mixture of pathologies manifesting in the postinjury brain. T₂-weighted imaging characterizes the lesion extent, hematomas, edema, and hippocampal and thalamic atrophy as well as morphologic details across the brain (Fig. 6A–G). Diffusion tensor imaging (DTI) probes the restricted movement of water molecules with a high spatial resolution and can be used to visualize the progression of structural changes in different hippocampal subfields for months after SE induced by systemic kainic acid or pilocarpine.⁶⁰ Increased fractional anisotropy in the dentate gyrus correlated with mossy fiber sprouting and reorganization of myelinated axons in the inner molecular layer.⁶⁰ Translatable advances in the imaging of the circuitry reorganization in epilepsy are expected from more advanced diffusion MRI techniques such as high angular resolution diffusion imaging (HARDI), and superior mapping of microhemorrhages, calcifications, and white matter damage is pursued by techniques probing local magnetic susceptibility differences, such as phase-imaging and quantitative susceptibility mapping.⁶¹ Altered networks are to be probed by combining functionality with structural information; manganese-enhanced MRI utilizing the activity-dependent uptake and axonal transport of Mn²⁺ can provide unique information about brain activation and structural connectivity, such as tracking layer specific thalamocortical connections and interhemispheric somatosensory connections⁶² as well as progressive mossy fiber sprouting.⁶³

Recent studies applying structural MRI have demonstrated proof-of-concept data that structural analysis can reveal patterns of structural abnormalities, which can be used as biomarkers for epileptogenesis. T₂ imaging of the amygdala and thalamus has shown promise in the search for biomarkers for epileptogenesis in an experimental model of

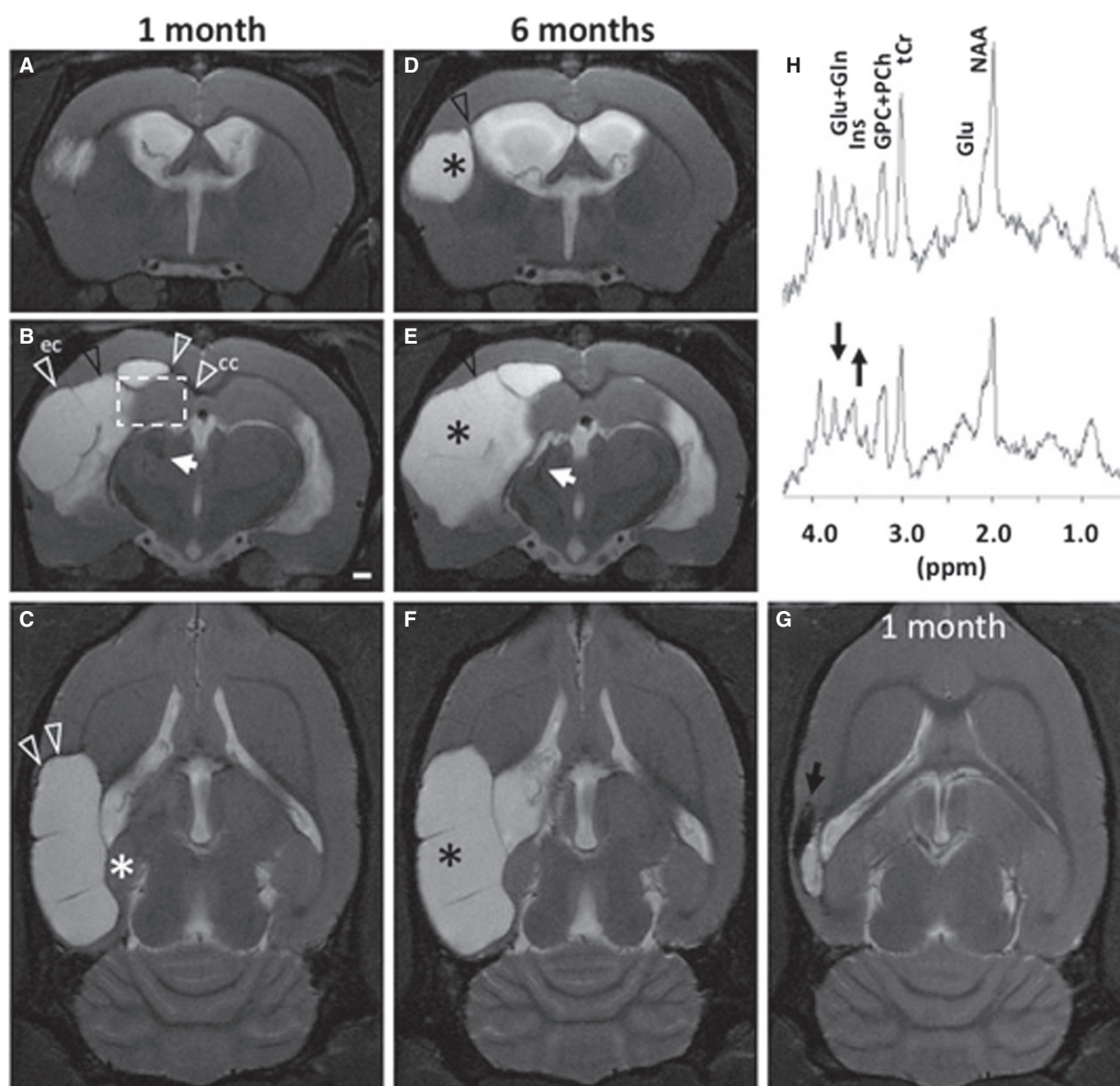


Figure 6.

Structural MRI and MRS of epileptogenesis after TBI that was induced with lateral fluid-percussion injury. (**A–C**) T₂-weighted coronal images (**A** rostral, **B** caudal, **C** horizontal) showing the extent of lesion at 1 month and (**D–F**) at 6 months post-TBI in the same rat. Note the progression of lesion, implying that the marker chosen can be a “moving target,” as its value can vary depending on the timing of the analysis. (**G**) Another animal with a substantially smaller, hemorrhagic lesion (black arrow) at 1 month post-TBI, indicating that even within the same animal cohort at a given time point there is variability between the animals, and different pathologic endophenotypes can be present (compare **C** and **G**). The panels also demonstrate the different pathologies that can serve as biomarkers for epileptogenesis and co-morbidogenesis; cortical lesion and atrophy (black asterisks in chronic state), enlarged ventricles, hippocampal atrophy (white asterisk), microbleeds associated with diffuse axonal injury in the external capsule (ec) and corpus callosum (cc), as well as along the lesion edge, (white arrowheads), and loss of white matter contrast (black arrowheads), and thalamic calcification-associated hypointensities (white arrows). (**H**) Representative MRS spectra of the ipsilateral hippocampus (dashed box in **B**, voxel size $3 \times 3 \times 2.5 \text{ mm}^3$) from a sham-operated (top) and an injured (bottom) animal at 5 months post-TBI. Levels of myo-inositol (Ins) were increased, whereas the levels of glutamate (Glu), N-acetylaspartylglutamate (NAAG), N-acetylaspartate + N-acetylaspartylglutamate (NAA + NAAG), and glutamate + glutamine (Glu + Gln) were decreased in injured animals (relative concentrations to total Cr, tCr; $p < 0.05$ as compared to controls). Levels of Ins, indicating gliosis, correlated with the memory impairment (latency in water maze, $r = 0.552$, $p < 0.001$) and levels of Glu + Gln correlated with seizure susceptibility (number of epileptiform discharges in pentylenetetrazol test, $r = -0.526$, $p < 0.05$). However, at 12 months post-TBI, receiver operating characteristic (ROC) or hierarchical clustering analyses indicated that these MRS markers had no value in diagnosis of memory impairment or increased seizure susceptibility. Scale bar equals 1 mm.

Epilepsia © ILAE

febrile seizures.⁶⁴ Another imaging study linked structural abnormalities assessed using T_2 , mean diffusivity D_{av} , and $T1\rho$ (i.e., T_1 in the rotating frame, a relaxation parameter that is sensitive to the extracellular matrix macromolecule content) in the thalamus and the cortex to increased seizure susceptibility in a model of posttraumatic epilepsy induced by lateral fluid-percussion injury.⁶³ In the same model, altered D_{av} in the hippocampus at acute and chronic time points after injury correlated both with seizure susceptibility and mossy fiber sprouting.⁶⁵ Finally, a reduced fractional anisotropy along the white matter of the temporal lobes quantified by DTI differentiated refractory from benign mesial TLE.⁶⁶

Rapidly developing molecular, structural, and functional imaging offers unforeseen possibilities to assess more accurately epileptogenesis-related changes in brain micro and macro circuits. Many of the new parameters obtained with novel techniques have not, however, yet been tested as biomarkers of epileptogenesis, even though it has been demonstrated that they show significant changes in epileptogenic focal areas in postinjury brain.

Clinical workflow: role of structural imaging in epilepsy patients

For humans, identifying an SOZ is a critical step in the presurgical workup of patients with epilepsy, as the odds of being seizure-free after surgery is 2.5 times greater when an epileptogenic lesion is seen on an MR scan. Thus, MRI is a mainstay in this workup. A critical first step is to obtain high-quality structural MR images using a standard epilepsy protocol as suggested by the ILAE.⁶⁷ These images must be reviewed by an expert in epilepsy imaging (e.g., neuroradiologist) who has been provided with all available clinical, EEG, and other imaging data (e.g., PET, SPECT). Despite best practice, 15–30% of patients with uncontrolled seizures have no visible lesion upon visual inspection of MR images.

If no epileptogenic lesion can be seen, further MR acquisitions and postprocessing methods can be used to identify such lesions. Important among these are quantification measures of hippocampal architecture, volume, and T_2 signal using methods such as shape analysis, volumetry, and T_2 relaxometry. Other new acquisition or postprocessing techniques such as voxel-based relaxometry, voxel-based morphometry, sulcal morphology, computational modelling (of cortical thickness, blurring, and tissue intensity), and diffusion imaging have been used to better identify malformations of cortical development and other abnormalities (Fig. 1). On average, these studies reported a 30–40% improvement in lesion detection rate over visual inspection of MR scans. Given that some of these methods can be very sensitive, there is also a possibility of false-positive results.

EEG-functional MRI

Scalp EEG-fMRI has been employed to identify blood oxygen level-dependent (BOLD) signal changes associated

with interictal epileptiform discharges (IEDs) with the hope of better defining the irritative and epileptogenic zones in focal epilepsy.

The BOLD response has been studied recently in a rat preclinical model of focal cortical dysplasia (FCD) with chronic seizures, where IED-evoked BOLD response networks comprised both cortical and subcortical structures with a rat-dependent topology.⁶⁸ In all rats, IEDs evoked both BOLD activation and deactivation. The authors also found that BOLD deactivation often had direct influences on areas with activation and it predicted topologic properties (i.e., focal/diffused, unilateral/bilateral) of the IED-evoked BOLD response network.⁶⁸ Song et al.⁶⁸ concluded that IEDs and disruptions in the resting state networks may be different manifestations of the same transient events, probably reflecting altered consciousness.

Most EEG-fMRI studies in humans have focused on IEDs rather than ictal discharges due to the unpredictability of occurrence of seizures. To this end, Zijlmans et al.⁶⁹ studied 29 patients initially rejected for epilepsy surgery and found that the BOLD response was co-localized with IED location in eight subjects. Scalp EEG-fMRI improved localization of the potential epileptogenic zone in four subjects and confirmed multifocality that supported the clinical decision not to offer surgery for some patients. EEG-fMRI has also improved clinical localization of the SOZ in patients with nonlesional frontal lobe epilepsy.⁷⁰ In another study, 33 patients underwent EEG-fMRI and 29 of 33 patients had BOLD response concordant with EEG localization; in 21 patients (64%), EEG-fMRI contributed to defining the SOZ.⁷¹ Furthermore, 12 of 14 patients had BOLD response localization that was validated by the presence of a structural MR abnormality or by subsequent intracranial recordings of seizures.

Several studies from two groups have shown that it is possible to perform simultaneous intracranial EEG-fMRI. These studies have shown very local BOLD signal changes associated with very focal IED recorded by intracranial EEG that are co-localized with the SOZ.^{72–74} In addition, remote BOLD signal changes were also seen with these focal IEDs, providing further insight into the epileptic networks in these subjects.

Few studies have correlated EEG-fMRI data with post-surgical outcomes. One report of 10 patients showed that in the 7 patients that were seizure-free following surgery, 6 of them had a strong concordance between the location of the IED-associated BOLD signal and tissue resection.⁷⁵ In the most comprehensive study to date,⁷⁶ 35 patients with focal epilepsy and a significant IED-associated BOLD response who underwent surgical resection were studied. Patients were classified into groups depending on the relationship between location of the maximal BOLD response and the surgical resection. The authors found that patients with surgical resection included the entirety of the maximal BOLD response was associated with a high sensitivity and positive

predictive value of a favorable post-operative outcome (87.5% and 70%, respectively).

Ictal EEG-fMRI studies are limited to case reports and case series due to challenge of capturing a seizure in the MR scanner. Such studies, although challenging, are especially useful when electrographic seizures⁷⁷ are recorded because these lacked significant motor manifestations that produce movement artifact. These studies have shown good concordance between the maximal BOLD response and the SOZ and have also provided insight into propagation patterns as well as preictal changes.⁷⁸

Arterial spin-labeling MRI

The SOZ is conventionally localized by EEG recordings of seizures or SPECT measures of blood flow during a seizure (ictal phase). However, EEG has limited localization accuracy, and ictal SPECT is very labor-intensive and costly. Evidence of a novel biomarker of the SOZ came from recent animal studies using an oxygen-sensing optrode that was implanted in the brain, demonstrating postictal hypoperfusion (up to 60% of baseline) at the SOZ, lasting up to 1 h.⁷⁹ In another preclinical study, cerebral blood flow was measured by arterial spin-labeling (ASL) MRI. The general approach taken by ASL is to modify the magnetization of arterial blood, to use this magnetically tagged blood as an endogenous tracer, and to measure the delivery of the tracer to target tissues. Cerebral blood flow was increased in the amygdala 2 and 14 days after pilocarpine-induced SE. This was associated with increased vessel density, which may explain this hyperperfusion, although the authors did not find any correlation between vessel density and amygdaloid cerebral blood flow.⁸⁰ In contrast, in humans, ASL MRI has demonstrated focal hypoperfusion interictally at the presumed SOZ in human subjects.⁸¹ In an ongoing study, ASL MRI has been used to measure perfusion in 15 patients to show that seizures are associated with postictal blood flow reductions (up to 60% of baseline) lasting up to 1 h, localized to the SOZ as defined by EEG and ictal SPECT, but with a better spatial resolution.⁸² Thus, ASL measurement of interictal and postictal hypoperfusion may represent a novel biomarker of the SOZ.

DO NO HARM—THE ROLE OF FUNCTIONAL IMAGING FOR PREDICTION OF POSTOPERATIVE COGNITIVE DEFICITS

Language

fMRI paradigms, including verbal fluency, verb generation, and semantic decision tasks, that activate anterior (Broca's area) and posterior (Wernicke's area) language areas, have been used to define typical and atypical language representation.⁸³ Individuals with left TLE and left language dominance recruit homologous right hemisphere

areas for language processing, suggesting widespread language representation.⁸⁴ Many factors affect language laterality and are associated with greater language shift to the right, like greater left-handedness, left-sided focus, and intermediate age at onset of epilepsy.⁸⁵ Concordance between MRI and the intracarotid Amytal (ICA) test is greatest for right TLE patients with left language dominance; and lowest for left TLE patients with left language dominance.⁸⁶ The consensus is that fMRI language lateralization can replace ICA test in most patients. The latter, however, may be required when a patient cannot perform the fMRI task, or if fMRI is contraindicated.⁸⁷

Preoperative verbal fluency fMRI activation in the middle and inferior frontal gyri predicts significant naming decline following left anterior temporal lobe resection (ATLR), with good sensitivity but poor specificity.⁸⁸ Auditory and visual naming paradigms may give more specific prediction of naming difficulties after ATLR.⁸⁹ When a cortical resection is needed close to eloquent language cortex, the localization inferred from language fMRI is not adequate to guide resection, and electrocortical stimulation and/or awake resections are usually undertaken.⁹⁰ An active area of current research is to determine whether noninvasive language mapping may render this unnecessary.

Memory

Memory impairment commonly accompanies TLE. Verbal memory encoding activates a bilateral network including temporal, parietal, and frontal lobes. Greater left hippocampal activation for word encoding is correlated with better verbal memory in patients with left TLE.⁹¹ Visual memory encoding recruits a more widespread bilateral cortical network and greater right hippocampal activation for face encoding is correlated with better visual memory in patients with right TLE.

Verbal and visual memory declines in one third of patients undergoing ATLR. Preoperative memory performance, age at onset of epilepsy, language lateralization, and asymmetry of activation on fMRI for verbal and visual memory can predict verbal memory decline in left ATLR but are less able to predict visual memory decline in right ATLR.⁹¹ Verbal memory encoding fMRI was the most consistent and discriminant between left and right TLE.⁹²

In left TLE, greater left than right anterior hippocampal activation on word encoding correlated with greater verbal memory decline after left ATLR, whereas greater left than right posterior hippocampal activation correlated with better postoperative verbal memory outcome. In right TLE, greater right than left anterior hippocampal functional MRI activation on face encoding predicted greater visual memory decline after right ATLR, whereas greater right than left posterior hippocampal activation correlated with better visual memory outcome. Preoperative memory activation was the strongest predictor of verbal and visual memory decline following ATLR, and preserved memory function

in the ipsilateral posterior hippocampus may help to maintain memory encoding after surgery.⁹¹

To be clinically relevant, fMRI paradigms have to predict outcome in the individual subject. A clinically applicable verbal memory fMRI paradigm that assessed lateralization index of memory, and associated language functions, in a medial temporal and frontal mask was the best predictor of verbal memory outcome after surgery in the dominant hemisphere in individual patients.⁹³

Working memory and functional connectivity analysis

Working memory is similarly affected as episodic memory in TLE, and improves after ATR, particularly left-sided. The sclerosed hippocampus is abnormally structurally and functionally connected, resulting in disruption of the normal segregation of the task-positive and task-negative networks, which support working memory is disrupted.⁹⁴ After left ATR, performance improved and greater deactivation of the left hippocampal remnant and the contralateral right hippocampus was observed, which suggests that working memory following surgery is dependent on the engagement of the posterior medial temporal lobes and eloquent cortex.⁹⁵ These studies suggest that the ability to activate or deactivate the ipsilateral posterior hippocampus is a reliable biomarker for the ability to cope postoperatively.

In summary, fMRI has a useful role in the presurgical assessment as a noninvasive predictive biomarker of language and memory decline after an ATR. Most of the studies report group findings, and the challenge remains to translate these findings to the prediction of outcome in the individual subject.

CONCLUSION

The development of structural and functional neuroimaging techniques has provided significant insights into the pathophysiologic mechanisms underlying epileptogenesis. We have reviewed animal and clinical studies that have identified potential biomarkers of epileptogenesis and ictogenesis including imaging markers of brain inflammation, metabolism, blood–brain barrier alterations as well as a number of MRS and structural/functional/blood flow MR markers of the irritative and SOZs.

In the future, we expect further developments that will improve on the sensitivity and specificity of imaging biomarkers of epileptogenesis and ictogenesis—for example, the structural and molecular imaging of epileptogenesis, using animal models of epilepsy with animals preselected for susceptibility to spontaneous seizures or drug responsiveness/resistance. This will be crucial for improving the ability to rapidly test new radioligands for PET and molecular imaging of the myriad of pathophysiologic processes underlying the genesis of seizures. In developing these markers, we must be mindful that the

mechanisms can occur simultaneously or in an ordered fashion. Targets could include markers of BBB breakdown, neuroinflammation, glial proliferation, neuronal dysfunction, metabolic dysfunction, synapses, or receptors. Similarly, advances in high-resolution structural and functional MRI (including resting state and EEG-fMRI), especially with higher field MR scanners, will allow further insights into the genesis and effects of seizures on the brain through studies of brain reorganization, changes in connectivity, and elucidation of epileptogenic networks underlying the generation of interictal and ictal discharges.

Recent advances in neuroimaging of ictogenesis and epileptogenic lesions has significantly improved the diagnosis and treatment of persons with epilepsy. As discussed herein, many of the imaging methodologies used in animals can be performed in humans. As such, the potential exists for clinical studies using patients preselected for increased risk of spontaneous seizures (e.g., following trauma, stroke, or other neurologic conditions) or for drug responsiveness in clinical trials. The development of patient cohorts such as these will all facilitate highly selective, cost-effective clinical trials. Thus, the significant potential exists for advanced neuroimaging methods to provide further insight into the genesis and effective treatment of epilepsy.

ACKNOWLEDGMENTS

This review is devised as extended account of the discussion that took place during the XIII WONOEP (Heybeliada Island, Istanbul, Turkey, August 31– to September 4, 2015) organized and supported by the Neurobiology Commission of the International League Against Epilepsy and generously sponsored by Harinarayan Family Foundation (U.S.A.) Cyberonics Inc.(U.S.A.), Insys Therapeutics Inc. (U.S.A.), Astellas Pharma (Japan), MSD (Japan), and Meiji Seika Pharma (Japan). We thank Prof. Jeroen Verhaeghe (Molecular Imaging Center Antwerp) for providing the rat FDG- and TSPO-PET scan images for Figure 2. Dr. Van Vliet is supported by the European Union's Seventh Framework Programme (FP7/2007–2013) under grant agreement no. 602102 (EPITARGET) and by the Dutch Epilepsy Foundation, project number 16-05. Dr. Dedeurwaerdere is supported by BOF UAntwerpen; The Research Foundation Flanders (FWO) (grant numbers 1.5.110.14N, G.038515N, and G.A009.13N); the Queen Elisabeth Medical Foundation for Neurosciences; and the European Union's Horizon 2020 research and innovation programme under the Marie Skłodowska-Curie grant agreement No 642881. Dr. H. Potschka is supported by Deutsche Forschungsgemeinschaft PO681/8-1. Dr. Pitkänen is supported by the European Union's Seventh Framework Programme (FP7/2007–2013) under grant agreement no 602102 (EPITARGET) and by Academy of Finland. Dr. Immonen is supported by Academy of Finland. Dr. Federico is supported by Canadian Institutes of Health Research (MOP-136839).

DISCLOSURE

None of the authors has any conflict of interest to disclose. We confirm that we have read the Journal's position on issues involved in ethical publication and affirm that this report is consistent with those guidelines.

REFERENCES

- Engel J Jr, Pitkanen A, Loeb JA, et al. Epilepsy biomarkers. *Epilepsia* 2013;54(Suppl. 4):61–69.

2. Pitkänen A, Engel J Jr. Past and present definitions of epileptogenesis and its biomarkers. *Neurotherapeutics* 2014;11:231–241.
3. Bouillere V, Boyet S, Marescaux C, et al. Mapping of the progressive metabolic changes occurring during the development of hippocampal sclerosis in a model of mesial temporal lobe epilepsy. *Brain Res* 2000;852:255–262.
4. Guo Y, Gao F, Wang S, et al. In vivo mapping of temporospatial changes in glucose utilization in rat brain during epileptogenesis: an 18F-fluorodeoxyglucose-small animal positron emission tomography study. *Neuroscience* 2009;162:972–979.
5. Shultz SR, Cardamone L, Liu YR, et al. Can structural or functional changes following traumatic brain injury in the rat predict epileptic outcome? *Epilepsia* 2013;54:1240–1250.
6. Kuhl DE, Engel J Jr, Phelps ME, et al. Epileptic patterns of local cerebral metabolism and perfusion in man: investigation by emission computed tomography of 18F-fluorodeoxyglucose and 13N-ammonia. *Trans Am Neurol Assoc* 1978;103:52–53.
7. Engel J Jr, Kuhl DE, Phelps ME. Patterns of human local cerebral glucose metabolism during epileptic seizures. *Science* 1982;218:64–66.
8. Goffin K, Dedeurwaerdere S, Van Laere K, et al. Neuronuclear assessment of patients with epilepsy. *Semin Nucl Med* 2008;38:227–239.
9. Fountain NB, Waldman WA. Effects of benzodiazepines on triphasic waves: implications for nonconvulsive status epilepticus. *J Clin Neurophysiol* 2001;18:345–352.
10. Fernandez-Torre JL, Solar DM, Astudillo A, et al. Creutzfeldt-Jakob disease and non-convulsive status epilepticus: a clinical and electroencephalographic follow-up study. *Clin Neurophysiol* 2004;115:316–319.
11. Struck AF, Westover MB, Hall LT, et al. Metabolic correlates of the ictal-interictal continuum: FDG-PET during continuous EEG. *Neurocrit Care* 2016;24(3):324–31.
12. Amhaoul H, Staelens S, Dedeurwaerdere S. Imaging brain inflammation in epilepsy. *Neuroscience* 2014;279:238–252.
13. Ji B, Maeda J, Sawada M, et al. Imaging of peripheral benzodiazepine receptor expression as biomarkers of detrimental versus beneficial glial responses in mouse models of Alzheimer's and other CNS pathologies. *J Neurosci* 2008;28:12255–12267.
14. Dedeurwaerdere S, Callaghan PD, Pham T, et al. PET imaging of brain inflammation during early epileptogenesis in a rat model of temporal lobe epilepsy. *EJNMMI Res* 2012;2:60.
15. Amhaoul H, Hamaide J, Bertoglio D, et al. Brain inflammation in a chronic epilepsy model: evolving pattern of the translocator protein during epileptogenesis. *Neurobiol Dis* 2015;82:526–539.
16. Brackhan M, Bascunana P, Postema JM, et al. Serial quantitative TSPO-targeted PET reveals peak microglial activation up to two weeks after an epileptogenic brain insult. *J Nucl Med* 2016;57(8):1302–1308.
17. Vezzani A, French J, Bartfai T, et al. The role of inflammation in epilepsy. *Nat Rev Neurol* 2011;7:31–40.
18. Martin A, Boisgard R, Kassiou M, et al. Reduced PBR/TSPO expression after minocycline treatment in a rat model of focal cerebral ischemia: a PET study using [(18)F]DPA-714. *Mol Imaging Biol* 2011;13:10–15.
19. Airas L, Dickens AM, Elo P, et al. In vivo PET imaging demonstrates diminished microglial activation after fingolimod treatment in an animal model of multiple sclerosis. *J Nucl Med* 2015;56:305–310.
20. Hirvonen J, Kreisl WC, Fujita M, et al. Increased in vivo expression of an inflammatory marker in temporal lobe epilepsy. *J Nucl Med* 2012;53:234–240.
21. Gershen LD, Zanotti-Fregonara P, Dustin IH, et al. Neuroinflammation in temporal lobe epilepsy measured using positron emission tomographic imaging of translocator protein. *JAMA Neurol* 2015;72:882–888.
22. Zanotti-Fregonara P, Zhang Y, Jenko KJ, et al. Synthesis and evaluation of translocator 18 kDa protein (TSPO) positron emission tomography (PET) radioligands with low binding sensitivity to human single nucleotide polymorphism rs6971. *ACS Chem Neurosci* 2014;5:963–971.
23. Bogdanovic RM, Syvanen S, Michler C, et al. (R)-[11C]PK11195 brain uptake as a biomarker of inflammation and antiepileptic drug resistance: evaluation in a rat epilepsy model. *Neuropharmacology* 2014;85:104–112.
24. Wanek T, Mairinger S, Langer O. Radioligands targeting P-glycoprotein and other drug efflux proteins at the blood-brain barrier. *J Labelled Comp Radiopharm* 2013;56:68–77.
25. Syvanen S, Eriksson J. Advances in PET imaging of P-glycoprotein function at the blood-brain barrier. *ACS Chem Neurosci* 2013;4:225–237.
26. Bartmann H, Fuest C, la Fougere C, et al. Imaging of P-glycoprotein-mediated pharmacoresistance in the hippocampus: proof-of-concept in a chronic rat model of temporal lobe epilepsy. *Epilepsia* 2010;51:1780–1790.
27. Syvanen S, Russmann V, Verbeek J, et al. [11C]quinidine and [11C]laniquidar PET imaging in a chronic rodent epilepsy model: impact of epilepsy and drug-responsiveness. *Nucl Med Biol* 2013;40:764–775.
28. Tournier N, Valette H, Peyronneau MA, et al. Transport of selected PET radiotracers by human P-glycoprotein (ABCB1) and breast cancer resistance protein (ABCG2): an in vitro screening. *J Nucl Med* 2011;52:415–423.
29. Romermann K, Wanek T, Bankstahl M, et al. (R)-[(11)C]verapamil is selectively transported by murine and human P-glycoprotein at the blood-brain barrier, and not by MRP1 and BCRP. *Nucl Med Biol* 2013;40:873–878.
30. Feldmann M, Asselin MC, Liu J, et al. P-glycoprotein expression and function in patients with temporal lobe epilepsy: a case-control study. *Lancet Neurol* 2013;12:777–785.
31. Koepp MJ. Neuroimaging of drug resistance in epilepsy. *Curr Opin Neurol* 2014;27:192–198.
32. Shin JW, Chu K, Shin SA, et al. Clinical applications of simultaneous PET/MR imaging using (R)-[11C]-verapamil with cyclosporin a: preliminary results on a surrogate marker of drug-resistant epilepsy. *AJNR Am J Neuroradiol* 2015;37:600–606.
33. Kreisl WC, Liow JS, Kimura N, et al. P-glycoprotein function at the blood-brain barrier in humans can be quantified with the substrate radiotracer 11C-N-desmethyl-loperamide. *J Nucl Med* 2010;51:559–566.
34. Kreisl WC, Bhatia R, Morse CL, et al. Increased permeability-glycoprotein inhibition at the human blood-brain barrier can be safely achieved by performing PET during peak plasma concentrations of tariquidar. *J Nucl Med* 2015;56:82–87.
35. Wanek T, Romermann K, Mairinger S, et al. Factors governing P-glycoprotein-mediated drug-drug interactions at the blood-brain barrier measured with positron emission tomography. *Mol Pharm* 2015;12:3214–3225.
36. Abbott NJ, Patabendige AA, Dolman DE, et al. Structure and function of the blood-brain barrier. *Neurobiol Dis* 2010;37:13–25.
37. van Vliet EA, Aronica E, Gorter JA. Blood-brain barrier dysfunction, seizures and epilepsy. *Semin Cell Dev Biol* 2015;38:26–34.
38. Marchi N, Granata T, Ghosh C, et al. Blood-brain barrier dysfunction and epilepsy: pathophysiologic role and therapeutic approaches. *Epilepsia* 2012;53:1877–1886.
39. Vazana U, Veksler R, Pell GS, et al. Glutamate-mediated blood-brain barrier opening: implications for neuroprotection and drug delivery. *J Neurosci* 2016;36(29):7727–7739.
40. Chassidim Y, Vazana U, Prager O, et al. Analyzing the blood-brain barrier: the benefits of medical imaging in research and clinical practice. *Semin Cell Dev Biol* 2015;38:43–52.
41. van Vliet EA, Otte WM, Gorter JA, et al. Longitudinal assessment of blood-brain barrier leakage during epileptogenesis in rats. A quantitative MRI study. *Neurobiol Dis* 2014;63:74–84.
42. Roch C, Leroy C, Nehlig A, et al. Magnetic resonance imaging in the study of the lithium-pilocarpine model of temporal lobe epilepsy in adult rats. *Epilepsia* 2002;43:325–335.
43. van Vliet EA, Otte WM, Wadman WJ, et al. Blood-brain barrier leakage after status epilepticus in rapamycin-treated rats I: magnetic resonance imaging. *Epilepsia* 2016;57:59–69.
44. van Vliet EA, Otte WM, Wadman WJ, et al. Blood-brain barrier leakage after status epilepticus in rapamycin-treated rats II: potential mechanisms. *Epilepsia* 2016;57:70–78.
45. Veksler R, Shelef I, Friedman A. Blood-brain barrier imaging in human neuropathologies. *Arch Med Res* 2014;45:646–652.
46. Chassidim Y, Veksler R, Lublinsky S, et al. Quantitative imaging assessment of blood-brain barrier permeability in humans. *Fluids Barriers CNS* 2013;10:9.

47. Tomkins O, Feintuch A, Benifla M, et al. Blood–brain barrier breakdown following traumatic brain injury: a possible role in posttraumatic epilepsy. *Cardiovasc Psychiatry Neurol* 2011;2011:765923.
48. Vezzani A, Friedman A. Brain inflammation as a biomarker in epilepsy. *Biomark Med* 2011;5:607–614.
49. Oz G, Alger JR, Barker PB, et al. Clinical proton MR spectroscopy in central nervous system disorders. *Radiology* 2014;270:658–679.
50. Duarte JM, Lei H, Mlynarik V, et al. The neurochemical profile quantified by in vivo 1H NMR spectroscopy. *NeuroImage* 2012;61:342–362.
51. Filibian M, Frasca A, Maggioni D, et al. In vivo imaging of glia activation using 1H-magnetic resonance spectroscopy to detect putative biomarkers of tissue epileptogenicity. *Epilepsia* 2012;53:1907–1916.
52. Connelly A, Jackson GD, Duncan JS, et al. Magnetic resonance spectroscopy in temporal lobe epilepsy. *Neurology* 1994;44:1411–1417.
53. Cross JH, Connelly A, Jackson GD, et al. Proton magnetic resonance spectroscopy in children with temporal lobe epilepsy. *Ann Neurol* 1996;39:107–113.
54. Achten E, Santens P, Boon P, et al. Single-voxel proton MR spectroscopy and positron emission tomography for lateralization of refractory temporal lobe epilepsy. *AJNR Am J Neuroradiol* 1998;19:1–8.
55. Kuzniecky R, Hugg J, Hetherington H, et al. Predictive value of 1H MRSI for outcome in temporal lobectomy. *Neurology* 1999;53:694–698.
56. Suhy J, Laxer KD, Capizzano AA, et al. 1H MRSI predicts surgical outcome in MRI-negative temporal lobe epilepsy. *Neurology* 2002;58:821–823.
57. Wellard RM, Briellmann RS, Prichard JW, et al. Myoinositol abnormalities in temporal lobe epilepsy. *Epilepsia* 2003;44:815–821.
58. Kuzniecky R, Hetherington H, Pan J, et al. Proton spectroscopic imaging at 4.1 tesla in patients with malformations of cortical development and epilepsy. *Neurology* 1997;48:1018–1024.
59. Freeman JL, Coleman LT, Wellard RM, et al. MR imaging and spectroscopic study of epileptogenic hypothalamic hamartomas: analysis of 72 cases. *AJNR Am J Neuroradiol* 2004;25:450–462.
60. Sierra A, Laitinen T, Grohn O, et al. Diffusion tensor imaging of hippocampal network plasticity. *Brain Struct Funct* 2015;220:781–801.
61. Lehto LJ, Sierra A, Corum CA, et al. Detection of calcifications in vivo and ex vivo after brain injury in rat using SWIFT. *NeuroImage* 2012;61:761–772.
62. Tucciarone J, Chuang KH, Dodd SJ, et al. Layer specific tracing of corticocortical and thalamocortical connectivity in the rodent using manganese enhanced MRI. *NeuroImage* 2009;44:923–931.
63. Immonen R, Kharatishvili I, Grohn O, et al. MRI biomarkers for post-traumatic epileptogenesis. *J Neurotrauma* 2013;30:1305–1309.
64. Choy M, Dube CM, Patterson K, et al. A novel, noninvasive, predictive epilepsy biomarker with clinical potential. *J Neurosci* 2014;34:8672–8684.
65. Kharatishvili I, Immonen R, Grohn O, et al. Quantitative diffusion MRI of hippocampus as a surrogate marker for post-traumatic epileptogenesis. *Brain* 2007;130:3155–3168.
66. Labate A, Cherubini A, Tripepi G, et al. White matter abnormalities differentiate severe from benign temporal lobe epilepsy. *Epilepsia* 2015;56:1109–1116.
67. Epilepsy CoNotILa. Recommendations for neuroimaging of patients with epilepsy. Commission on Neuroimaging of the International League Against Epilepsy. *Epilepsia* 1997;38:1255–1256.
68. Song Y, Sanganahalli BG, Hyder F, et al. Distributions of irritative zones are related to individual alterations of resting-state networks in focal epilepsy. *PLoS ONE* 2015;10:e0134352.
69. Zijlmans M, Huiskamp G, Hersevoort M, et al. EEG-fMRI in the preoperative work-up for epilepsy surgery. *Brain* 2007;130:2343–2353.
70. Moeller F, Tyvaert L, Nguyen DK, et al. EEG-fMRI: adding to standard evaluations of patients with nonlesional frontal lobe epilepsy. *Neurology* 2009;73:2023–2030.
71. Pittau F, Dubeau F, Gotman J. Contribution of EEG/fMRI to the definition of the epileptic focus. *Neurology* 2012;78:1479–1487.
72. Aghakhani Y, Beers CA, Pittman DJ, et al. Co-localization between the BOLD response and epileptiform discharges recorded by simultaneous intracranial EEG-fMRI at 3 T. *NeuroImage Clin* 2015;7:755–763.
73. Cunningham CB, Goodyear BG, Badawy R, et al. Intracranial EEG-fMRI analysis of focal epileptiform discharges in humans. *Epilepsia* 2012;53:1636–1648.
74. Vuillimoz S, Carmichael DW, Rosenkranz K, et al. Simultaneous intracranial EEG and fMRI of interictal epileptic discharges in humans. *NeuroImage* 2011;54:182–190.
75. Thornton R, Laufs H, Rodionov R, et al. EEG correlated functional MRI and postoperative outcome in focal epilepsy. *J Neurol Neurosurg Psychiatry* 2010;81:922–927.
76. An D, Fahoum F, Hall J, et al. Electroencephalography/functional magnetic resonance imaging responses help predict surgical outcome in focal epilepsy. *Epilepsia* 2013;54:2184–2194.
77. LeVan P, Tyvaert L, Moeller F, et al. Independent component analysis reveals dynamic ictal BOLD responses in EEG-fMRI data from focal epilepsy patients. *NeuroImage* 2010;49:366–378.
78. Chaudhary UJ, Carmichael DW, Rodionov R, et al. Mapping preictal and ictal haemodynamic networks using video-electroencephalography and functional imaging. *Brain* 2012;135:3645–3663.
79. Teskey GC, Farrell JS. Brief seizures induce a severe ischemic/hypoxic episode. *Epilepsia* 2012;53:104–105.
80. Hayward NM, Nodde-Ekane XE, Kutchiashvili N, et al. Elevated cerebral blood flow and vascular density in the amygdala after status epilepticus in rats. *Neurosci Lett* 2010;484:39–42.
81. Pendse N, Wissmeyer M, Altrichter S, et al. Ictal arterial spin-labeling MRI perfusion in intractable epilepsy. *J Neuroradiol* 2010;37:60–63.
82. Singh S, Gaxiola-Valdez I, Sandy S, et al. Prolonged post-ictal cerebral hypoperfusion detected by arterial spin labelling (ASL) MRI – a possible replacement for ictal SPECT? *Epilepsia* 2015;56:16.
83. Abbott DF, Waites AB, Lillywhite LM, et al. fMRI assessment of language lateralization: an objective approach. *NeuroImage* 2010;50:1446–1455.
84. Jensen EJ, Hargreaves IS, Pexman PM, et al. Abnormalities of lexical and semantic processing in left temporal lobe epilepsy: an fMRI study. *Epilepsia* 2011;52:2013–2021.
85. Berl MM, Zimmaro LA, Khan OI, et al. Characterization of atypical language activation patterns in focal epilepsy. *Ann Neurol* 2008;75:33–42.
86. Benke T, Koyle B, Visani P, et al. Language lateralization in temporal lobe epilepsy: a comparison between fMRI and the Wada Test. *Epilepsia* 2006;47:1308–1319.
87. Wagner K, Hader C, Metternich B, et al. Who needs a Wada test? Present clinical indications for amobarbital procedures. *J Neurol Neurosurg Psychiatry* 2012;83:503–509.
88. Bonelli SB, Powell RH, Yogarajah M, et al. Imaging memory in temporal lobe epilepsy: predicting the effects of temporal lobe resection. *Brain* 2012;133:1186–1199.
89. Rosazza C, Ghielmetti F, Minati L, et al. Preoperative language lateralization in temporal lobe epilepsy (TLE) predicts peri-ictal, pre- and post-operative language performance: an fMRI study. *NeuroImage Clin* 2013;3:73–83.
90. Mathern GW, Beninsig L, Nehlig A. From the editors: epilepsy's survey on the necessity of the Wada test and intracranial electrodes for cortical mapping. *Epilepsia* 2014;55:1887–1889.
91. Bonelli SB, Powell RH, Yogarajah M, et al. Imaging memory in temporal lobe epilepsy: predicting the effects of temporal lobe resection. *Brain* 2010;133:1186–1199.
92. Towgood K, Barker GJ, Caceres A, et al. Bringing memory fMRI to the clinic: comparison of seven memory fMRI protocols in temporal lobe epilepsy. *Hum Brain Mapp* 2015;36:1595–1608.
93. Sidhu MK, Stretton J, Winston GP, et al. Memory fMRI predicts verbal memory decline after anterior temporal lobe resection. *Neurology* 2015;84:1512–1519.
94. Stretton J, Winston GP, Sidhu M, et al. Disrupted segregation of working memory networks in temporal lobe epilepsy. *NeuroImage Clin* 2013;2:273–281.
95. Stretton J, Sidhu MK, Winston GP, et al. Working memory network plasticity after anterior temporal lobe resection: a longitudinal functional magnetic resonance imaging study. *Brain* 2014;137:1439–1453.